CHEMISTRY OF MATERIALS

ARTICLE

pubs.acs.org/cm

Strong Red-Emitting near-Infrared-to-Visible Upconversion Fluorescent Nanoparticles

Guangshun Yi,[†] Yanfen Peng,[†] and Zhiqiang Gao[‡,*]

[†]Institute of Bioengineering and Nanotechnology, 31 Biopolis Way, The Nanos, Singapore 138669

[‡]Department of Chemistry, National University of Singapore, 3 Science Drive 3, Singapore 117543

Supporting Information

ABSTRACT: Near infrared (NIR)-to-red upconversion fluorescent nanoparticles of yttrium oxyfluoride, ytterbium, erbium/yttrium oxyfluoride (YOF:Yb,Er/YOF) with a core/shell structure have been prepared for the first time. Under 980 nm NIR excitation, they emitted strong red upconversion fluorescence with a sharp emission band topping at ~669 nm. Compared with the most efficient green emitting hexagonal phase $NaYF_4$:Yb,Er upconversion fluorescent nanoparticles, our red-emitting fluorescent nanoparticles exhibited even stronger fluorescence. The YOF shell played a dual-role in the upconversion: it greatly enhanced the red emission at ~669 nm (~18 times) and suppressed the green emission of erbium at ~530 nm. These nanoparticles were rendered hydrophilic by using several strategies and were further conjugated to antibodies for cancer cell labeling and imaging. As both excitation and emission were in the long wavelength range (>650 nm), which are transparent to tissues, along with their strong and narrow emission, these red emission upconversion fluorescent nanoparticles offer excellent opportunities for biosensing and in vivo bioimaging applications.

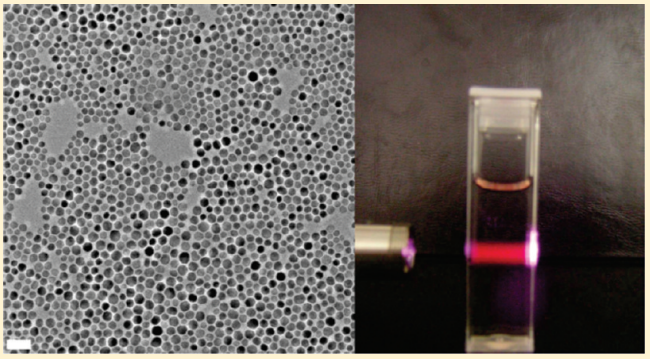

KEYWORDS: yttrium oxyfluoride, upconversion fluorescence, nanoparticles, core/shell, bioimaging

Near infrared (NIR)-to-visible upconversion fluorescent nanoparticles are materials that convert NIR excitation into visible emission.[1] Compared to fluorescent organic dyes and quantum dots, upconversion fluorescent nanoparticles are photostable, contain nontoxic elements, NIR excitation with sharp visible emission peaks, and the absence of auto fluorescence in biological specimens. These nanoparticles are ideal fluorescent probes for biological detection and imaging.[2,3] So far, 980 nm NIR-to-green $NaYF_4$:Yb,Er and NIR-to-blue $NaYF_4$:Yb,Tm nanoparticles have been prepared by us and other groups using different approaches.[4−12] Among them, the most efficient upconversion fluorescent material is the hexagonal phase $NaYF_4$:Yb,Er (20%Yb and 2% Er), which emits green light at ~540 nm upon 980 nm NIR excitation.

As fluorescent probes, more emission colors of nanoparticles with high fluorescent efficiencies are desirable for multiplexed detection and imaging. Efforts have been devoted to develop more emission colors of upconversion fluorescent nanoparticles. For example, Wang et al. recently reported a nice work on multiple emission colors of $NaYF_4$ nanoparticles, by codoping of Er and Tm, and/or modulating the doping levels.[13] In this way, they can tune the upconversion emission colors from blue to NIR. Although good successes have been achieved in these studies, it is still challenging to apply these nanoparticles as potentially high-performance fluorescent probes in biological studies, due mainly to (i) the emission colors are tuned by mixing of multiple emissions mainly from the blue emission of thulium (Tm), green and red emission of erbium (Er). For bioapplications like biosensing, nanoparticles with a single color emission are highly desirable. (ii) The nanoparticles are in cubic phase, compared with their desirable hexagonal phase $NaYF_4$, the upconversion fluorescence efficiency is very low and in the following order: blue emission $NaYF_4$:Yb,Tm (cubic phase) ≪ green emission $NaYF_4$:Yb,Er (cubic phase) ≪ green emission $NaYF_4$:Yb,Er (hexagonal phase). Nann et al. has first demonstrated four color emissions from $NaYbF_4$ doped with Tm, Ho, Er, and Yb, respectively.[14] They are however still less efficient compared to the most efficient $NaYF_4$:Yb,Er nanoparticles. And each of the four colors actually comprises multiple emission peaks rather than a single one.

In this work, we reported on the preparation of non-$NaYF_4$-based yttrium oxyfluoride, ytterbium, erbium/yttrium oxyfluoride, (YOF:Yb,Er/YOF) core/shell-structured upconversion fluorescent nanoparticles. The nanoparticles were prepared via a modified procedure of thermolysis of rare earth trifluoroacetates.[7,15,16] Characteristic to upconversion materials, it was observed that under 980 nm NIR excitation, the nanoparticles gave out intense red light with an emission band topping at 669 nm. Our

Received: November 5, 2010
Revised: April 8, 2011
Published: May 09, 2011

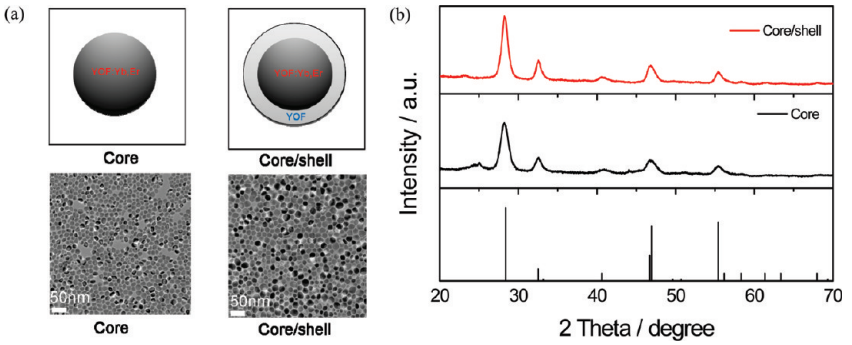

Figure 1. (a) TEM images of YOF:Yb,Er core, and YOF:Yb,Er/YOF core/shell nanoparticles. Precursor molar ratio of core:shell = 1:1. (b) XRD spectra of YOF:Yb,Er core, and YOF:Yb,Er/YOF core/shell nanoparticles.

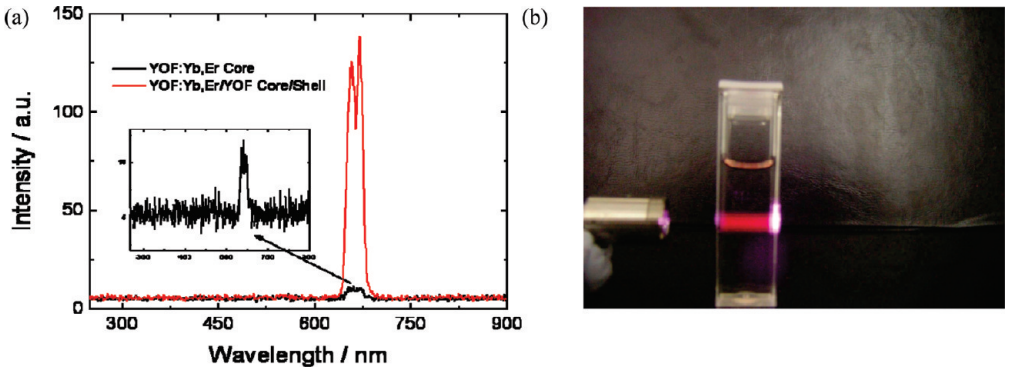

Figure 2. (a) Upconversion fluorescence of the YOF:Yb,Er core and the YOF:Yb,Er/YOF core/shell nanoparticles. Excitation = 980 nm NIR. Emission slit = 3 nm. (b) YOF:Yb,Er/YOF nanoparticles in cyclohexane. With 980 nm NIR excitation, the nanoparticles gave off intense red emission fluorescence.

upconversion fluorescence from the YOF:Yb,Er/YOF nanoparticles is, surprisingly, stronger than the green-emitting hexagonal phase $NaYF_4$:Yb,Er. The nanoparticles were further rendered hydrophilic, conjugated with anti-Her2 antibodies, and cultured with cancer cells for cancel cell imaging. It was found that the nanoparticles with antibody conjugation selectively attached themselves onto cancer cells, whereas nanoparticles without antibody conjugation were not able to recognize the cancer cells.

RESULTS AND DISCUSSION

Morphology and Structure of the Nanoparticles. Figure 1a shows transmission electron microscopic (TEM) and X-ray diffraction (XRD) results of the synthesized YOF:Yb,Er and YOF:Yb,Er/YOF nanoparticles. The molar ratio for core:shell was 1:1. The size of the core was 15 ± 0.4 nm and the size of the core/shell nanoparticles was 18 ± 0.7 nm, estimated from counting 100 particles from five TEM micrographs. From the Scherer's equation, the calculated particle sizes for core was 14 and 17 nm for core/shell, respectively. From the XRD spectra in Figure 1b, the structure of the nanoparticles was confirmed to be cubic phase yttrium oxide fluoride (YOF), in accordance with JCPDS No. 00−038−0746.

Upconversion Fluorescence of the Nanoparticles. Figure 2 shows room-temperature upconversion fluorescence spectra of the YOF:Yb,Er core and YOF:Yb,Er/YOF core/shell (core:shell = 1:1) nanoparticles. The emission band topped at ∼669 nm, comprising at least two emission peaks with a full width at half-maximum (fwhm) of ∼20 nm. This emission was attributed to $^4F_{9/2}$ to $^4I_{15/2}$ transitions of erbium.[1] From the fluorescence measurements, it can be seen that the emission from the core is very weak. However, after growing the shell on the core, the fluorescence intensity was increased by ∼18.5 times. As the nanoparticle size was only enlarged by 3 nm from 15 to 18 nm after growing the shell, the fluorescence enhancement is unlikely from the particle size change. More probably, it originates from the elimination of surface fluorescence quenching because erbium on the particle's surface will not or only gives very weak fluorescence due to surface quenching.[17,20,21] The YOF shell effectively isolates the core from interaction with solvent, significantly suppresses the surface quenching, and therefore greatly enhances the upconversion fluorescence. The effect of shell on upconversion fluorescence will be further discussed in the following section, Shell Effect on the Upconversion Fluorescence.

The nanoparticles were easily dispersed in aprotic solvents like cyclohexane, toluene, and chloroform to form homogeneous and transparent colloidal solutions. This suggests that the nanoparticle surface is coated with the long chain ligand of oleylamine. Figure 2b shows the YOF:Yb,Er/YOF nanoparticles in cyclohexane. The nanoparticles were completely and homogeneously dispersed, forming a clear suspension. Intense upconversion fluorescence was seen upon 980 nm NIR excitation (Figure 2b).

The red upconversion fluorescence of the YOF:Yb,Er/YOF nanoparticles was compared with the hexagonal phase green emitting $NaYF_4$:Yb,Er nanoparticles. We used the $NaYF_4$:Yb,Er nanoparticles as our bench mark as they are widely used and have

dx.doi.org/10.1021/cm103175s |Chem. Mater. 2011, 23, 2729–2734

been regarded as one kind of the most efficient upconversion nanoparticles. The hexagonal phase $NaYF_4$:Yb,Er was prepared using two reported methods[7,22] with a composition of $NaY_{0.78}F_4$:$Yb_{0.2}$,$Er_{0.02}$, and were coated with oleylamine and oleic acid ligand on their surfaces, respectively. The composition of our red emitting nanoparticles was $Y_{0.78}$OF:$Yb_{0.2}$,$Er_{0.02}$/0.5YOF (core:shell = 1:0.5). For comparison, samples contain similar amounts of Yb and Er (20 μM Yb and 2 μM Er, determined by ICP-MS) were dispersed in equal volumes of cyclohexane for fluorescence testing. In both cases our red emission nanoparticles exhibited stronger upconversion fluorescence than the green emitting $NaYF_4$:Yb,Er nanoparticles (Figure 3). It was worth noting that in our case, the upconversion fluorescence efficiency follows the order of YOF:Yb,Er/0.5YOF < YOF:Yb,Er/YOF < YOF:Yb,Er/2YOF. The thicker the shell, the stronger the upconversion fluorescence as discussed in the following section.

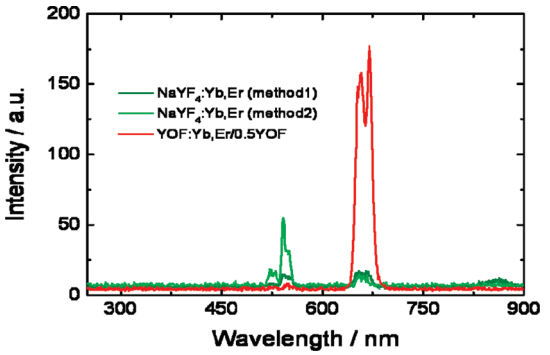

Figure 3. Emission spectra of cyclohexane solutions of the YOF:Yb,Er/0.5 YOF core/shell nanoparticles and two green emitting hexagonal phase $NaYF_4$:Yb,Er nanoparticles containing similar amounts of Yb and Er (20 μM Yb and 2 μM Er) under identical experimental conditions.

Growth Mechanism of the Nanoparticles. To study the growth mechanism of the nanoparticles, after raising the precursor solution temperature to 300 °C, we took aliquots of the reaction mixture at different time intervals for TEM and fluorescence characterizations. Figure 4a shows TEM micrographs of nanoparticles after the reaction temperature was kept at 300 °C for 0 to 10 h, respectively. As seen in Figure 4a, the nanoparticles became bigger and bigger from 0 to 1 h. Between 2 and 5 h, the nanoparticles became stabilized in size. However, a mixture products of YOF:Yb,Er nanoparticles and YOF:Yb,Er nanorods were obtained when the reaction was kept at 300 °C for a prolonged period of time.

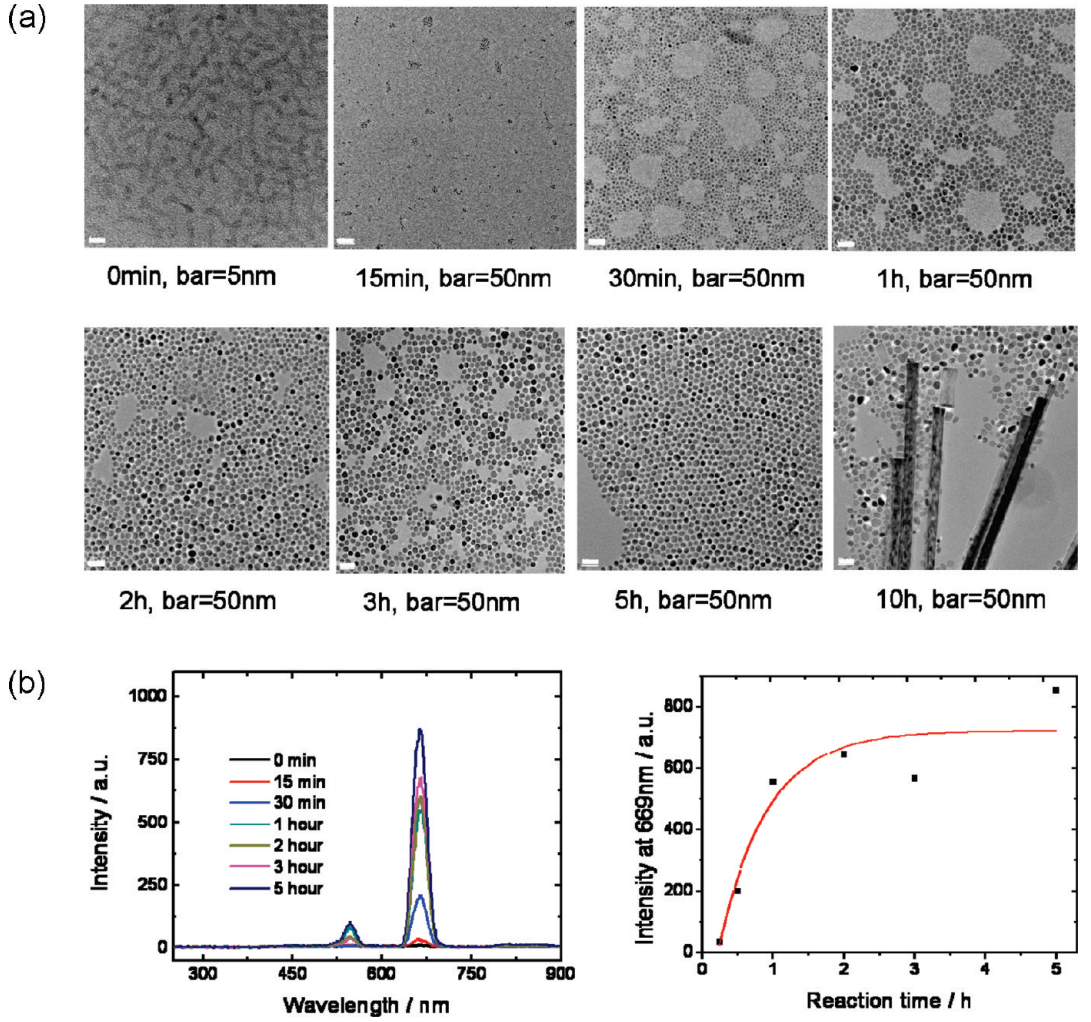

Figure 4. (a) YOF:Yb,Er nanoparticle formation at 300 °C for 0 to 10 h. (b) Fluorescent spectra of YOF:Yb,Er nanoparticles growing at 300 °C for 0−5 h and the corresponding plot of fluorescent intensities at 669 nm vs reaction time.

dx.doi.org/10.1021/cm103175s |*Chem. Mater.* 2011, 23, 2729–2734

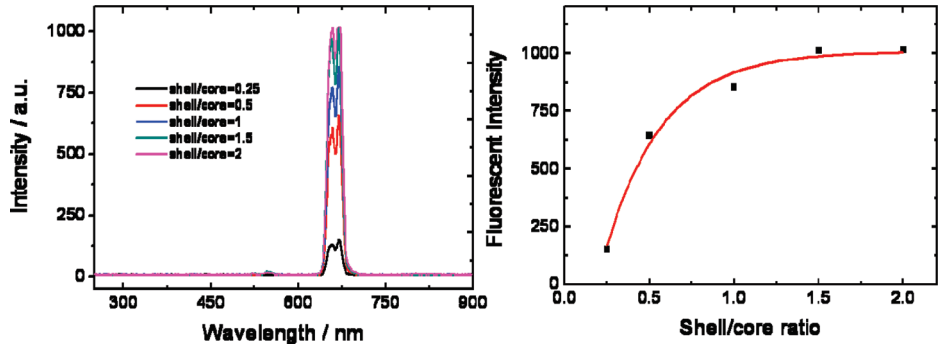

Figure 5. (a) Upconversion fluorescent spectra of YOF:Yb,Er/YOF core/shell nanoparticles with shell to core molar ratio of 0.25:2. (b) Shell thickness effect on upconversion fluorescence intensity.

Figure 4b is the corresponding upconversion fluorescence spectra of the core nanoparticles that reacted at 300 °C from 0 to 5 h. As depicted in Figure 4b, two emission bands at 669 nm (red) and 540 nm (green) respectively were observed with an intensity ratio of ~1/9 (green/red). From 0 to 1 h, the upconversion fluorescent intensities increased quickly as a result of nanoparticle growth. After 1 h, the upconversion fluorescence intensities continued to increase but at a much slower pace, mainly due to the improvement in crystal quality, rather than the particle size growth. The fluorescent results are consistent with our TEM observations.

Shell Effect on the Upconversion Fluorescence. The YOF shell plays an important role in the upconversion fluorescence of the YOF:Yb,Er/YOF core/shell nanoparticles. Without the shell protection, the red upconversion fluorescence was very weak. In contrast, after growing the shell, significant upconversion fluorescence was observed. Even growing a very thin layer of YOF (0.25 times) led to a significant enhancement in the red fluorescence. To study the effect of the shell thickness on the upconversion fluorescence enhancement, we have prepared different core/shell nanoparticles with shell/core precursor molar ratio varying from 0.25 to 2. Figure 5 shows the fluorescence spectra of the nanoparticles tested under the same experimental conditions. When the shell became thicker and thicker, from 0.25 to 1.5, the red upconversion fluorescence became stronger and stronger, and leveled off from 1.5 to 2 (Figure 5).

It is also very interesting to note that, contrary to the two emission bands (green and red) observed for the core nanoparticles (Figure 4b), there's only one emission band comprising at least 2 peaks centered at ~669 nm (Figure 5a) for the YOF:Yb, Er/YOF core/shell nanoparticles. This suggests a dual-function of the YOF shell, enhancing the red emission band at ~669 nm and suppressing the green emission band at~540 nm.

To understand this dual-function of the YOF shell, we used the intensity ratio of the red/green emissions (R/G) to study the shell function. We speculated that the increase in the R/G ratio is due to host (matrix) effect of YOF. As the YOF:Yb,Er nanoparticles is small (~15 nm), a large number of Er ions are on the nanoparticle surface. And, the Er ions on the surface have a lower R/G ratio than that of the Er ions in the center of the YOF host, probably due to surface quenching of the red emission.[17,20,21] After growing the YOF shells onto the YOF:Yb,Er core nanoparticles, the host effect was largely enhanced, resulting in a much improved R/G ratio. If this hypothesis holds, the R/G ratio should be exclusively correlated to the particle size: The smaller the nanoparticles, the more the Er ions on the surface, and the lower the R/G ratio; or vise versa. As we already have YOF:Yb,Er core nanoparticles of different sizes from the same reaction batch during the preparation of the core/shell nanoparticles (Figure 4), the R/G ratios were estimated for the 3-nm (ripening for 0 min in the solution at 300 °C), 7-nm nanoparticles (15 min ripening), and 13-nm YOF:Yb,Er nanoparticles (1 h ripening). It was found that a steady increase in the R/G ratio is observed with the growth of the nanoparticles. For example, the 3 nm nanoparticles had an R/G ratio of 1.66, the 7-nm ones had an R/G ratio of 5.56, and an R/G ratio of 7.4 was found for the 13 nm nanoparticles.

To further confirm this host effect, we prepared some bulk YOF:20%Yb,2%Er phosphor, following a published procedure.[23] The XRD pattern of the phosphor (see Figure S3 in the Supporting Information) indicates that the bulk YOF:20% Yb,2%Er phosphor has the same crystal structure as the YOF: Yb,Er nanoparticles. Because there was only a very small portion of Er ions located on the surface, the bulk YOF:Yb,Er phosphor had a very intense red emission band at ~669 nm without any detectable green emission (see Figure S4 in the Supporting Information), affirming the beneficial effect of the YOF host, favoring the red emission and retarding the green emission.

YOF:Yb,Er/YOF Nanoparticles for Cancer Cell Imaging. The as prepared YOF:Yb,Er/YOF nanoparticles are hydrophobic with oleylamine on their surfaces. For biological applications, nanoparticles with hydrophilic surfaces are more desirable. In our experiments, we used three methods to convert the nanoparticles water dispensable, with particle surfaces functionalized with carboxyl, and amine groups, respectively.

To render the nanoparticles hydrophilic with carboxyls on their surfaces, we used octylamine and isopropylamine neutralized poly(acrylic acid) (PAA) as a coating material.[17] The amphiphilic block copolymer was absorbed onto the nanoparticle surfaces through hydrophobic attraction between the original oleylamine ligand on the particle surfaces and the hydrophobic chain of the polymer. The hydrophilic carboxyls of the polymer permit aqueous dispersion and further bioconjugation. From our experiments, we found that when the PAA/nanoparticles was >25/1 (1 mg of nanoparticles with 25 mg of PAA), a clear aqueous solution of nanoparticles was obtained (see the Supporting Information), while when the PAA/nanoparticles ratio was <10/1, turbid dispersions of the nanoparticles persisted.

To introduce amines onto the nanoparticles, we used branched poly (ethylene amine) (PEI) to replace the original oleylamine on the particle surfaces. The amount of PEI to nanoparticles and exchange time are the two key factors to make

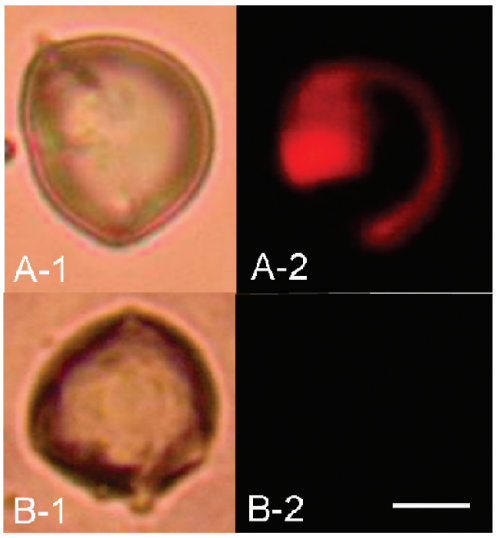

Figure 6. Imaging of cancer cells via recognition of cancer marker Her2 with the nanoparticles. (A-1) Bright-field and (A-2) 980 nm NIR excited images of SK-BR-3 cancer cells incubated with the anti-Her2 antibody conjugated nanoparticles. (B-1) Bright-field and (B-2) 980 nm NIR excited images of SK-BR-3 cancer cells incubated with nanoparticles without antibody conjugation. Scale bar = 10 μm.

stable hydrophilic nanoparticles. In our study, 150 mg of PEI in chloroform was mixed with 1 mg of the nanoparticles. Stable water suspensions of the nanoparticles were only obtainable after at least 7 days of incubation (see the Supporting Information). Different from the PAA coated nanoparticles mentioned above, here PEI replaces the original oleylamine on the nanoparticle surfaces via ligand exchange. Excessive amount of PEI with prolonged incubation time enables the exchange to be complete. Another method to bestow the nanoparticles hydrophilic with amine is by silica coating using a reverse-microemulsion method.[18] TEM tests showed that each particle was coated with a silica shell (see the Supporting Information). By using a mixture of tetraethyl orthosilicate (TEOS) and 3-aminopropyltriethoxysilane (APTES), silica-coated nanoparticles with terminated amine were obtained and were water-soluble (see the Supporting Information).

Some cancer cells have an overexpressed protein called Her2 on their surfaces. To image them, anti-Her2 antibody was first conjugated to the nanoparticles through covalent bonding (experimental section) and the nanoparticles were then incubated with SK-BR-3 cancer cells. For comparison, nanoparticles without any antibody conjugation were also incubated with the same cancer cells. As shown in Figure 6, under a modified epifluorescence microscope, the cancer cell incubated with the antibody-conjugated nanoparticles showed a strong fluorescence pattern as a direct result of Her2 recognition, whereas virtually no fluorescence was detected for the cancer cells incubated with the nanoparticles without antibody conjugation.

CONCLUSIONS

In summary, we have developed a simple thermolysis procedure for synthesizing strong red-emitting upconversion fluorescent YOF:Yb,Er/YOF core/shell nanoparticles. Fluorometric tests indicated that when excited by 980 nm NIR light, the YOF:Yb,Er/YOF nanoparticles display ultrabright red emission with a narrow emission band at ~669 nm, which is much more intensive than that of the best upconversion nanoparticles under the same conditions. The excellent optical properties of the YOF:Yb,Er/YOF nanoparticles are related to their structural uniqueness and imply potential applications in bioimaging and biosensing. Because both excitation and emission are in the long wavelength range, which are transparent to tissues, plus their strong and single color emission, the nanoparticles are also very attractive for in vivo applications.

METHODS

Materials. Rare earth oxide (Y_2O_3, Yb_2O_3, Er_2O_3), trifluoroacetic acid (CF_3COOH), Na_2CO_3, $NaIO_4$, ammonium hydroxide solution, cyclohexane, oleylamine, PEI (branched with MW ~25,000) were from Sigma-Aldrich and used without further purification. YCl_3, $YbCl_3$, and $ErCl_3$ stock solutions were prepared by dissolving respective rare earth oxides in HCl, drying at elevated temperatures to evaporate water and the excessive HCl, and dissolving in water as stock solutions. Anti-Her2 antibody was from Zoolem Marketing.

Preparation of Rare Earth Trifluoacetate Stock Solutions. The precursor stock solution of rare earth trifluoroacetates ($Y_{0.78}Yb_{0.2}Er_{0.02}(CF_3COO)_3$) for core: To an aqueous solution comprising of 11.7 mL of 0.2 M YCl_3 were added 3 mL of 0.2 M $YbCl_3$, 0.3 mL of 0.2 M $ErCl_3$ (Y:Yb:Er = 78:20:2, molar ratio), and 2 mL of 25% ammonium hydroxide. White precipitate of rare earth hydroxides formed immediately. The precipitate was washed with water 5 times to remove chloride and the excessive ammonium hydroxide. The precipitate was then dissolved in 2 mL of CF_3COOH and a clear solution of rare earth trifluoroacetates was formed. The solution was dried at 100 °C to produce rare earth trifluoroacetate salts. They were then dissolved in 12 mL of oleylamine and kept as stock solution. This solution contained a total of 3 mmol rare earth trifluoroacetates in 12 mL of oleylamine, equivalent to 0.25 mmol/mL in concentration. The yttrium trifluoroacetate stock solution ($Y(CF_3COO)_3$) for shell: This procedure was the same as that used to prepare the core precursor solution, except that 15 mL of 0.2 M YCl_3 was used in stead of a mixture of YCl_3, $YbCl_3$ and $ErCl_3$.

Synthesis of YOF:Yb,Er Core and YOF:Yb,Er/YOF Core/Shell Nanoparticles. Briefly, in a 25 mL three-necked flask, 4 mL of oleylamine and 1 mL of the core precursor (0.25 mmol) solution were mixed. Under vigorous magnetic stirring, the temperature of the solution was raised to 150 °C. Vacuum was applied to remove water residue until no bubbles came out from the reaction mixture. A clear solution was obtained after this procedure. Under a blanket of N_2 protection in the flask, the temperature of the solution was raised and kept at 300 °C for 2 h. The solution remained clear during heating. When the reaction was completed, the temperature was cooled down to 100 °C, where the solution became turbid as the result of nanoparticles being separated from the solution. Some aliquots of the solution were kept as reference of YOF:Yb,Er core nanoparticles and used for further characterization.

To form the YOF:Yb,Er/YOF core/shell-structured nanoparticles (e.g., core:shell = 1:1), 1 mL of the shell stock solution was added into the above core solution. The temperature was again raised to 150 °C, and use vacuum to remove the water residue in the reaction mixture. Under N_2 protection, the temperature of the reaction mixture was raised and remained at 300 °C for 1 h to grow the YOF shells onto the core nanoparticles. Then, the mixture was cooled down to room temperature and stored in a sealed vial for further characterizations and applications. By changing the core/shell precursor volume ratios, different thicknesses of the YOF shells can be introduced onto the cores.

Water-Soluble PAA Coated YOF:Yb,Er/YOF Nanoparticles. Referring to a published procedure,[17] coating the nanoparticles with PAA was achieved as follows: 100 μL of the YOF:Yb,Er/YOF nanoparticle stock solution was centrifuged at 10K rpm for 5 min. The precipitate was

rinsed with ethanol for 3 times and redispersed in 2 mL of chloroform. Coating solution was prepared by dissolving 25 mg octylamine and isopropylamine neutralized PAA in 2 mL of chloroform. The two solutions were mixed and slowly dried in a fume hood, after which the PAA was coated onto the nanoparticle surfaces through hydrophobic−hydrophobic interaction. The PAA-coated nanoparticles were first dispersed in ethanol and purified by centrifugation and redispersion. Finally, they were dispersed in 2 mL of pH 8.2 10 mM borate buffer.

Water-Soluble PEI-Coated YOF:Yb,Er/YOF Nanoparticles. Again, 100 μL of the YOF:Yb,Er/YOF nanoparticle stock solution was centrifuged at 10K rpm for 5 min. The precipitate was rinsed with ethanol for 3 times and redispersed in 2 mL of chloroform. PEI coating solution was prepared by dissolving 150 mg of PEI in 2 mL of chloroform. The two solutions were mixed and stirred for at least 7 days under ambient conditions. Afterward, 8 mL of cyclohexane was added to the reaction mixture to precipitate the PEI coated nanoparticles. The PEI coated nanoparticles were collected by centrifugation, and dried in vacuum for overnight to remove cyclohexane and chloroform residues. They were then purified by multiple centrifugation−dispersion cycles in 2 mL of water.

Water-Soluble Silica Coated YOF:Yb,Er/YOF Nanoparticles. A literature procedure was adopted in the preparation of the silica coated YOF:Yb,Er/YOF nanoparticles.[18] Igepal CO-520 (0.8 g, 2 mmol) was dissolved in 10 mL of cyclohexane. Three mg of the YOF:Yb,Er/YOF nanoparticles predissolved in 1 mL of cyclohexane was added to the Igepal CO-520 solution to form a transparent reverse microemulsion. Aliquots of 10 μL of 28% ammonium hydroxide, 40 μL of TEOS, and 10 μL of APTES were added sequentially. And the mixture was gently stirred for 20 h at room temperature. The resulting YOF:Yb,Er/YOF @ SiO_2−NH_2 nanoparticles were precipitated by adding 2 mL of acetone and were collected by centrifugation at 4000 rpm for 5 min. The collected nanoparticles were dispersed in ethanol and further purified by multiple centrifugation-dispersion cycles.

Conjugation of YOF:Yb,Er/YOF Core/Shell Nanoparticles with Antibody. To couple antibody onto the nanoparticles, 100 μL of 1 mg/mL anti-Her2 antibody was first treated with 10 μL of 100 mM $NaIO_4$ for 30 min in the darkness.[19] The antibody was then diluted by pH 7.4 phosphate-buffered saline (PBS) and incubated with the amine-bound YOF:Yb,Er/YOF nanoparticles for 1 h. Unbounded antibody was removed by centrifugation and washing. The antibody-conjugated nanoparticles were kept in PBS.

Characterization. TEM bright-field images of the nanoparticles were collected on a FEI Tecnai F20 transmission electron microscope using a 200 kV accelerating. Specimens were prepared by slowly vaporizing a drop of the nanoparticle dispersion in cyclohexane on a Formvar carbon-coated copper grid. Selected area electron diffraction pattern (SAED) was taken with a camera length of 76 cm. XRD spectra were acquired with a PANalytical X-ray diffractometer (X'pert PRO), with Cu Kα radiation at 1.5406 Å. Samples were prepared by vaporizing nanoparticle hexane solutions onto zero-background XRD holders (silicon base). Upconversion fluorescence spectra were obtained on a Shimadzu RF-5301 photoluminescence spectrometer, with an external 980-nm laser diode (1 W, continuous wave with 1 m fiber, Beijing Viasho Technology Co., Beijing.) as the excitation source, in place of the xenon lamp in the spectrometer. The spectrometer operated with excitation slit at 0 nm, and emission slit at 3, 5, and 10 nm, respectively. Clear YOF:Yb, Er core and/or YOF:Yb,Er/YOF dispersions in cyclohexane were used for the fluorescence tests, respectively.

Cancer Cell Imaging. Human breast cancer cell line SK-BR-3 was cultured (37 °C, 5% CO_2) on a chambered glass slide. For the detection of Her2 on the cells, SK-BR-3 cells were fixed with 4% formaldehyde for 10 min and blocked for 20 min in PBS containing 1% (wt/vol) BSA. A aliquot of PBS solution containing anti-HER2 antibody conjugated nanoparticles was applied to the SK-BR-3 cells and incubated for 30 min at 37 °C. Fluorescence imaging was acquired with an epifluorescent microscope (Carl Zeiss, Axiostar plus) equipped with a 980 nm NIR fiber laser and a CCD camera (Canon power shot A620). The emissions were collected through a broad pass filter in the wavelength of 400−800 nm.

■ ASSOCIATED CONTENT

Supporting Information. Characterization and derivations of the upconversion fluorescent nanoparticles. This material is available free of charge via the Internet at http://pubs.acs.org.

■ AUTHOR INFORMATION

Corresponding Author

*E-mail: chmgaoz@nus.edu.sg. Tel: 6516-3887. Fax: 6779-1691.

■ ACKNOWLEDGMENT

This work was funded by Agency for Science, Technology and Research (A*STAR).

■ REFERENCES

(1) Auzel, F. *Chem. Rev.* **2004**, *104*, 139.
(2) van de Rijke, F.; Zijlmans, H.; Li, S.; Vail, T.; Raap, A. K.; Niedbala, R. S.; Tanke, H. J. *Nat. Biotechnol.* **2001**, *19*, 273.
(3) Lim, S. F.; Riehn, R.; Ryu, W. S.; Khanarian, N.; Tung, C. K.; Tank, D.; Austin, R. H. *Nano Lett.* **2006**, *6*, 169.
(4) Heer, S.; Kompe, K.; Gudel, H. U.; Haase, M. *Adv. Mater.* **2004**, *16*, 2102.
(5) Yi, G. S.; Lu, H. C.; Zhao, S. Y.; Yue, G.; Yang, W. J.; Chen, D. P.; Guo, L. H. *Nano Lett.* **2004**, *4*, 2191.
(6) Mai, H.-X.; Zhang, Y.-W.; Si, R.; Yan, Z.-G.; Sun, L.-d.; You, L.-P.; Yan, C.-H. *J. Am. Chem. Soc.* **2006**, *128*, 6426.
(7) Yi, G. S.; Chow, G. M. *Adv. Funct. Mater.* **2006**, *16*, 2324.
(8) Boyer, J. C.; Cuccia, L. A.; Capobianco, J. A. *Nano Lett.* **2007**, *7*, 847.
(9) Li, Z. Q.; Zhang, Y. *Angew. Chem., Int. Ed.* **2006**, *45*, 7732.
(10) Chen, Z.; Chen, H.; Hu, H.; Yu, M.; Li, F.; Zhang, Q.; Zhou, Z.; Yi, T.; Huang, C. *J. Am. Chem. Soc.* **2008**, *130*, 3023.
(11) Li, Z.; Zhang, Y.; Jiang, S. *Adv. Mater.* **2008**, *20*, 4765.
(12) Wang, X.; Zhuang, J.; Peng, Q.; Li, Y. D. *Nature* **2005**, *437*, 121.
(13) Wang, F.; Liu, X. G. *J. Am. Chem. Soc.* **2008**, *130*, 5642.
(14) Ehlert, O.; Thomann, R.; Darbandi, M.; Nann, T. *ACS Nano* **2008**, *2*, 120.
(15) Zhang, Y.-W.; Sun, X.; Si, R.; You, L.-P.; Yan, C.-H. *J. Am. Chem. Soc.* **2005**, *127*, 3260.
(16) Du, Y. P.; Zhang, Y. W.; Sun, L. D.; Yan, C. H. *J. Phys. Chem. C* **2008**, *112*, 405.
(17) Yi, G. S.; Chow, G. M. *Chem. Mater.* **2007**, *19*, 341.
(18) Selvan, S. T.; Tan, T. T.; Ying, J. Y. *Adv. Mater.* **2005**, *17*, 1620.
(19) Kumar, S.; Aaron, J.; Sokolov, K. *Nat. Protocols* **2008**, *3*, 314.
(20) Abel, K. A.; Boyer, J. C.; van Veggel, F. *J. Am. Chem. Soc.* **2009**, *131*, 14644.
(21) Mai, H. X.; Zhang, Y. W.; Sun, L. D.; Yan, C. H. *J. Phys. Chem. C* **2007**, *111*, 13721.
(22) Liu, C.; Wang, H.; Li, X.; Chen, D. *J. Mater. Chem.* **2009**, *19*, 3546.
(23) Holsa, J.; Kestila, E. *J. Alloys Compd.* **1995**, *225*, 89.